A semi-mechanistic model for partitioning evapotranspiration reveals transpiration dominates the water flux in drylands

E. G. Reich[1], K. Samuels-Crow[1], J. B. Bradford[2], M. Litvak[3], D. R. Schlaepfer[2,4], and K. Ogle[1,5]

[1] School of Informatics, Computing, and Cyber Systems, Northern Arizona University, Flagstaff, AZ, USA.

[2] United States Geological Survey, Northwest Climate Adaptation Science Center & Southwest Biological Science Center, Flagstaff, AZ, USA.

[3] Department of Biology, University of New Mexico, Albuquerque, NM, USA.

[4] Center for Adaptable Western Landscapes, Northern Arizona University, Flagstaff, AZ, USA.

[5] Center of Ecosystem Science and Society, Northern Arizona University, Flagstaff, AZ, USA.

Corresponding author: Emma Reich (egr65@nau.edu)

Key Points:

- A new evapotranspiration partitioning model (DEPART) was developed using eddy covariance flux tower measurements in a Bayesian framework
- This method produces daily estimates of transpiration and weekly estimates of plant water-use efficiency at the ecosystem scale
- This method reveals water-use efficiency is limited by moisture supply in more arid climates and moisture demand in less arid climates

Abstract

Popular evapotranspiration (ET) partitioning methods make assumptions that might not be well-suited to dryland ecosystems, such as high sensitivity of plant water-use efficiency (WUE) to vapor pressure deficit (VPD). Our objectives were to (1) create an ET partitioning model that can produce fine-scale estimates of transpiration (T) in drylands, and (2) use this approach to evaluate how climate controls T and WUE across ecosystem types and timescales along a dryland aridity gradient. We developed a novel, semi-mechanistic ET partitioning method using a Bayesian approach that constrains abiotic evaporation using process-based models, and loosely constrains time-varying WUE within an autoregressive framework. We used this method to estimate daily T and weekly WUE across seven dryland ecosystem types and found that T dominates ET across the aridity gradient. Then, we applied cross-wavelet coherence analysis to evaluate the temporal coherence between focal response variables (WUE and T/ET) and environmental variables. At yearly scales, we found that WUE at less arid, higher elevation sites was primarily limited by atmospheric moisture demand, and WUE at more arid, lower elevation sites was primarily limited by moisture supply. At sub-yearly timescales, WUE and VPD were sporadically correlated. Hence, ecosystem-scale dryland WUE is not always sensitive to changes in VPD at short timescales, despite this being a common assumption in many ET partitioning models. This new ET partitioning method can be used in dryland ecosystems to better understand how climate influences physically and biologically driven water fluxes.

Plain Language Summary

We developed a new model to better understand how plants use and lose water in drylands and applied it to seven dryland sites. Our model partitions evapotranspiration— the total water lost to the atmosphere from the Earth's surface— into its components. Evapotranspiration consists of both evaporation from wet surfaces, such as wet soil, and the water lost from plants when they photosynthesize. Currently, models assume a strong relationship between the efficiency with which plants use water ("water-use efficiency") and the dryness of the atmosphere, but this violates what we know about how plants function in drylands. For example, in drylands many plants are adapted to very dry conditions and their water use can be less sensitive to increasing atmospheric dryness compared to plants from wet environments. Using this new model, we found that plant water-use efficiency is only correlated with atmospheric dryness some of the time and that evapotranspiration is primary controlled by water lost from plants. This model allows us to better understand the importance of timescale and ecosystem type in governing plant water-use dynamics and more accurately assess the potential impact of changing climate conditions on dryland water fluxes and ecosystem processes.

1 Introduction

On an ecosystem scale, quantifying the importance of plants in governing evaporative water loss remains challenging. Towards addressing this challenge, eddy covariance flux towers offer a powerful methodology for quantifying the magnitude and variability in ecosystem water and energy fluxes in addition to carbon fluxes (Baldocchi, 2014). Flux towers provide NEE (i.e., net ecosystem exchange, or the net CO_2 flux) and evapotranspiration (i.e., ET, or the loss of water from an ecosystem to the atmosphere) data products. While there are well-tested methods that partition NEE into its components (i.e., gross primary productivity [GPP] and ecosystem respiration), and that have been integrated into standard flux tower data processing (Desai et al., 2008; Reichstein et al., 2005), accurate and widely applicable methods for partitioning ET into evaporation and transpiration are still being developed (Baldocchi, 2020; Stoy et al., 2019). However, understanding ET and its components is essential to evaluating the contribution of plants to ecosystem water fluxes and for improving land surface models.

ET consists of two distinct evaporative processes: the abiotic process of evaporation (E) and the biotic process of transpiration (T). From an atmospheric perspective, T and E both describe the physical process by which liquid water changes to water vapor (Miralles et al., 2020). From an ecosystem perspective, T differs from E in that T is regulated by plant biological processes. In particular, T is affected by leaf-level physiology and is linked to GPP through plant stomatal conductance, which controls both plant photosynthesis and plant water loss. The magnitude of T is governed by soil water availability and plant responses to environmental variables, such as stomata closing in response to high vapor pressure deficit (VPD) or opening in response to increased soil moisture availability (Beer et al., 2009).

Partitioning flux tower estimates of ET into E and T can help connect individual plant adaptive strategies to ecosystem-level water balance across ecosystem types. However, estimating E and T can be complicated because the relative importance of environmental drivers can differ between E and T (Sun et al., 2019). Moreover, the timescales over which environmental drivers influence E and T likely vary. By representing partitioned ET as the contribution of T to ET (i.e., T/ET) we can assess the influences of climatic and biological drivers on ecosystem water fluxes (Gan & Liu, 2020; Tarin et al., 2020) and better understand the processes giving rise to temporal and spatial variation in these fluxes. Several studies have evaluated patterns of T/ET over different timescales (e.g., following rain pulses, seasonally, or annually), but the results are somewhat inconsistent (Moran et al., 2009). For example, global T/ET estimates vary between 24% to 90% depending on the ET partitioning method used (Wei et al., 2017).

In recent years, there have been notable advances in developing models that partition ET using flux tower data that can be applied to a broad range of ecosystem types (Eichelmann et al., 2022; Li et al., 2019; Nelson et al., 2018; Pérez-Priego et al., 2018; Scanlon et al., 2019; Scott & Biederman, 2017; Zahn et al., 2022; Zhou et al., 2016). However, previous ET partitioning models have various potential issues when applied to dryland ecosystems. For example, they estimate water-use efficiency (WUE) using only dry periods (Nelson et al., 2018; Zhou et al., 2016), assume plants maximize carbon gain per unit water lost (Pérez-Priego et al., 2018; Zhou et al., 2016), or do not produce daily estimates or E, T, or WUE (Scott & Biederman, 2017) (see Table 1). Due to these limitations, a flux tower-based ET partitioning approach is needed that can be confidently applied to dryland ecosystems.

Plant WUE, the ratio of carbon gained to water lost during photosynthesis, connects the water and carbon cycles. Constraining WUE has been the main focus of improving ET partitioning models (Niu et al., 2011). Some flux-based ET partitioning models—such as the models introduced in Pérez-Priego et al. (2018) and Zhou et al. (2016)—use theories of stomatal behavior related to leaf-level (intrinsic) WUE to estimate WUE at the ecosystem scale. Essentially, these methods assume that plants maximize carbon gain per unit water lost; i.e., they assume stomata are sensitive to VPD and will close rapidly in response to increasing VPD to avoid further drops in plant water potential (Jarvis & McNaughton, 1986). However, it is unclear what conditions need to be met at the ecosystem scale for this assumption to hold (Stoy et al., 2019), as plant communities have a range of adaptive strategies related to water use and water stress (Dong et al., 2020; Engelbrecht et al., 2007; Maherali et al., 2004). The relationship between plant carbon gain and water loss can vary across spatial and temporal scales (Feng et al., 2022; Gomarasca et al., 2023; Lin et al., 2018). Moreover, the assumption of stomatal sensitivity to VPD may not be appropriate when considering ecosystems such as drylands, which support plants that vary greatly along the iso/anisohydry continuum, or that are strongly anisohydric (i.e., stomata are relatively insensitive to changes in VPD) (Guo et al., 2020; Ogle et al., 2012).

Table 1
Summary of existing eddy covariance flux tower ET partitioning methods.

Approach and source	**Assumptions potentially not suited to drylands**
uWUE (Zhou et al., 2016)	WUE is calculated during dry periods when T/ET ≈ 1. WUE is optimized according to changes in VPD.
Scott and Biederman (Scott & Biederman, 2017)	Suited to drylands, but only applicable to monthly timescales. E is invariant across years per month.
Transpiration Estimation Algorithm (TEA) (Nelson et al., 2018)	WUE is calculated during dry periods when T/ET ≈ 1.
Perez-Priego (Perez-Priego et al., 2018)	WUE is optimized according to changes in VPD.
Conductance Partitioning (Li et al., 2019)	Intercepted E is negligible; understory T is negligible; canopy conductance is proportional to GPP.
Flux-Variance Partitioning (FVS) (Scanlon et al., 2019, 2019; Skaggs et al., 2018)	Leaves are the only main source/sink for CO_2 and H_2O fluxes. Requires prior knowledge of plant WUE or assumes optimality.
Conditional Eddy Covariance (Zahn et al., 2022)	Assumes scalar similarity of turbulence.
Eichelmann (Eichelmann et al., 2022)	Nighttime water fluxes are exclusively E.

To address these limitations, we developed the Dynamic Evapotranspiration Partitioning Approach for Rapid Timescales (DEPART), a semi-mechanistic ET partitioning approach.

Table 2
Summary of eddy covariance sites used in this study.

	Site	Vegetation type	Elevation (m)	MAP (mm)	MAT (°C)	% Sand	% Clay
Low elevation	US-Seg	Desert grassland	1622	273	13.67	88.67	4.32
	US-Ses	Desert shrubland	1593	273	13.72	74.46	6.29
Mid elevation	US-Wjs	Juniper savanna	1931	361	15.2	87	2.55
	US-Mpj	Piñon-juniper woodland	2196	385	10.5	56.74	9.51
High elevation	US-Vcp	Ponderosa pine woodland	2500	550	9.8	71.48	5.24
	US-Vcm	Burned subalpine mixed conifer forest	3000	646	6.4	72.35	3.55
	US-Vcs	Unburned subalpine mixed conifer forest	2752	551	4.6	79.64	2.51

Note. In 2013, a fire burned US-Vcm, and we only use the data from 2014 onwards. It is worth noting that since this is a recovering mixed conifer forest, US-Vcm is primarily dominated by elderberry shrubs during this period.

Essentially, DEPART partitions ET by constraining E, a primarily abiotic process, rather than constraining WUE using physiological theories, and therefore forgoing stomata sensitivity assumptions. DEPART uses a Bayesian framework to utilize the underlying principles and structure of the linear model presented in Scott and Biederman (2017). DEPART, however, is applied at much faster time-scales representative of the temporal dynamics of E and T, facilitated by a modeling framework that integrates constraints on E and WUE. Thus, DEPART can inform our current understanding of underlying plant water-use processes in water-limited ecosystems.

Using this new model, DEPART, we asked: (1) how does T/ET and WUE vary across dryland ecosystem types and (2) how does the relationship between T/ET and WUE versus environmental variables vary at different temporal scales across dryland ecosystem types? To address these questions, we used the DEPART framework to estimate E and T at daily scales and WUE at weekly scales over multiple years across seven dryland ecosystem types. We then used cross-wavelet coherence analysis to evaluate the temporal relationships between T/ET and environmental variables and between WUE and environmental variables.

2 Methods

2.1 Eddy Covariance Flux Data

In this study, we used eddy covariance flux tower data from the New Mexico Elevation Gradient (NMEG), a network of seven Ameriflux sites spanning an elevation and aridity gradient in New Mexico (USA) that offer long-term measurements (~2008-2020) of carbon, water, and energy fluxes in dominant ecosystem types present in the southwestern USA (Table 2). Briefly, these NMEG sites include a desert grassland (US-Seg), desert shrubland (US-Ses), juniper savannah (US-Wjs), piñon-juniper woodland (US-Mpj), ponderosa pine forest (US-Vcp), burned mixed conifer forest (US-Vcm), and unburned mixed conifer forest (US-Vcs). The strategic distribution of NMEG sites (Table 2) allows us to ask questions using flux towers across multiple biomes (Anderson-Teixeira et al., 2011). All sites have sandy loam soils. Detailed site descriptions can be found in Anderson-Teixeira et al. (2011) and Samuels-Crow et al. (2020).

Site data were processed from freely available datasets at daily resolution from the Ameriflux website (https://ameriflux.lbl.gov/); these data include ET, estimated GPP partitioned from NEE (Reichstein et al., 2005), and meteorological measurements. While we recognize that GPP is not measured directly and estimated via NEE partitioning algorithms, we assume that the GPP estimates are fairly accurate given that the partitioning approaches have been repeatedly tested, refined, and generally accepted by the flux community. Volumetric soil water content (SWC) data were collected every 30 minutes using probes (Campbell Scientific CS610 at US-Mpj; Campbell Scientific CS616 at all other sites) across four pits at each site and processed following Rüdiger et al. (2010), then averaged to daily values.

2.2 Soil Water Content Gap-Filling

At flux tower sites, SWC data can be missing for various reasons, including sensor malfunctions or interference from animals and weather (Baldocchi et al., 2001). Across sites, daily SWC data gaps ranged from 2.14% to 21.60% of all daily SWC data, with average gap sizes varying from 15 to 36 days. To fill gaps in the daily SWC data to better estimate soil E, we applied a simple systematic gap-filling approach. To gap-fill missing SWC, we linearly interpolated SWC sequentially for days in which there were no precipitation events, using the SWC values reported at the start and end of the gap. The SOILWAT2 model was used to estimate missing SWC during gap periods that received precipitation. SOILWAT2 is a process-based, multiple soil layer simulation model of ecosystem water balance that has been validated in several dryland ecosystems (Bradford et al., 2014, 2020; Bradford & Lauenroth, 2006; Schlaepfer et al., 2017). Daily SWC values simulated by SOILWAT2 were linearly regressed against known flux tower site SWC, and the linear equation was used to correct for magnitude discrepancies in the SOILWAT2 SWC data. The adjusted SOILWAT2 values were used to gap-fill the missing SWC data when linear interpolation would be less appropriate, such as after a large precipitation pulse. To test the gap-filling approach, we artificially introduced gaps into the observed data and applied the technique to see how closely the simulated data matched the observed data that were removed. The R^2 (coefficient of determination) values from a regression of observed on simulated data ranged from 0.71 (US-Vcm) to 0.88 (US-Ses).

2.3 Soil Property Analysis

When considering E, soil texture is particularly important because it controls the surface area available for water particles to bond to and the amount of pore space that could store water (Komatsu, 2003; Lee & Pielke, 1992). To determine soil texture properties for each site, we collected site-specific soil samples from each NMEG tower site in the summer of 2021. We collected soil samples from 0-5 cm from 1-3 holes (3 holes each at US-Seg, US-Vcp, US-Vcm, and US-Vcs and 1 hole each at US-Ses, US-Wjs, and US-Mpj). From these separate samples, we determined the percentages of sand, silt, and clay using the hydrometer technique (Garcia Coronado et al., 2008), which was then used to calculate the soil clay and sand percentages and soil field capacity for each sample. This information improved soil model parameters affecting soil E and accounted for landscape heterogeneity within each flux tower footprint (see section 2.4).

2.4 The DEPART Model for ET Partitioning

The DEPART model structure builds on the framework developed by Scott and Biederman (2017). Briefly, the original Scott and Biederman approach predicts monthly T and E based on a regression of monthly values of ET on GPP obtained for multiple years, where the intercept in this regression, E', is interpreted as the physical-based evaporation term for a given month. The DEPART model, however, can be applied at finer temporal scales (daily to weekly) by constraining E' with process-based, nonlinear evaporation equations. While the DEPART method is structurally similar to the approach of Scott and Biederman (2017), the latter method assumes E'= E is invariant across years for each month. The DEPART E estimate, however, can vary by day, so E'= E without assuming a lack of variance in E.

Incorporation of these additional models and data (constraints on E' and WUE) are accommodated within a Bayesian framework. Consequently, $\mathrm{WUE}^{\mathrm{DEPART}}$, a key term in the model, is allowed to vary with time, and we allow $\mathrm{WUE}^{\mathrm{DEPART}}$ to vary at weekly scales to capture the influence of rainy periods. The modeled $\mathrm{WUE}^{\mathrm{DEPART}}$ does not rely on the concept that plants maximize carbon gain per unit water lost or that WUE is tightly coupled to VPD, and it does not require previous knowledge of plant stomatal physiological responses.

DEPART uses daily carbon (GPP) and water (ET) fluxes from eddy covariance flux towers to partition ET, based on linear regressions of ET versus GPP where, for each day, *d*, and week, *w*, associated with each day, *w*(*d*):

$$ET_d = m_{w(d)} GPP_d + E'_d \tag{1}$$

where the slope, m, represents the inverse of the weekly WUE. Here, E'_d, is the intercept that denotes ET when GPP = 0, representing the condition when plants are inactive (i.e., GPP = 0, so expect T = 0). Note that equation 1 is distinct from Scott and Biederman (2017) because ET, GPP, and E are allowed to vary by day and the slope is allowed to vary by week. Following equation 1, daily transpiration, T_d, is estimated as,

$$T_d = m_{w(d)} GPP_d \tag{2}$$

Therefore, m represents an inverse WUE index such that $1/m = \mathrm{WUE}^{\mathrm{DEPART}}$, which is expected to roughly match weekly estimates of GPP/T. $\mathrm{WUE}^{\mathrm{DEPART}}$—and hence, $m = 1/\mathrm{WUE}^{\mathrm{DEPART}}$ in equations (1) and (2)—is loosely constrained by a stochastic autoregressive model that assigns a hierarchical prior to each weekly $\mathrm{WUE}^{\mathrm{DEPART}}$ value, given the prior week's $\mathrm{WUE}^{\mathrm{DEPART}}$ value such that:

$$WUE_w^{DEPART} \sim Normal(WUE_{w-1}^{DEPART}, \sigma_{WUE}^2) \tag{3}$$

Again, *w* indicates the week. Within the Bayesian framework, the standard deviation, σ_{WUE}, is assigned a uniform prior such that $\sigma_{WUE} \sim Uniform(0,20)$. Essentially, the estimated WUE^{DEPART} varies around the WUE^{DEPART} of the previous week with some unknown variance, and all weekly WUE^{DEPART} values and the unknown variance are estimated by fitting the full DEPART model to the eddy flux tower data. In other words, WUE is a stochastic quantity in DEPART, and it is estimated to "optimize" the relationship in equation 1. Thus, a novel aspect of DEPART is that WUE^{DEPART} is stochastic and its temporal variation is weakly constrained by the above autoregressive model and equation 1.

Unique to the DEPART model, both E' and WUE^{DEPART} are constrained, but to differing degrees. In contrast to the weak constraints on weekly WUE^{DEPART}, daily E' is relatively tightly constrained by mechanistic equations for physical-based soil and intercepted E based on models in the Community Land Model (CLM) versions 3.5 and 4.5 (Oleson et al., 2013), succinctly summarized in Merlin et al. (2016). In particular, DEPART models soil E as a mixture of two common equations. The first is based on the soil surface resistance (r_{ss}) and α formulations used in CLM 3.5, which give the following for *LE*, the latent energy:

$$LE(r_{ss}, \alpha) = \frac{\rho C_p}{\gamma} \cdot \frac{\alpha e_{sat}(T_{soil}) - e_a}{r_{ah} + r_{ss}} \tag{4}$$

And the second is based on the β and α formulations used in CLM 4.5:

$$LE(\beta, \alpha) = \beta \cdot \frac{\rho C_p}{\gamma} \cdot \frac{\alpha e_{sat}(T_{soil}) - e_a}{r_{ah}} \tag{5}$$

For simplicity of presentation, we avoid subscripting with *d* in equations (4) and (5), but LE does vary by day, *d*, because several terms vary by day, including: the density of air (ρ), saturated vapor pressure in the soil (e_{sat}), soil temperature (T_{soil}), saturated air vapor pressure (e_a), aerodynamic resistance to heat transfer (r_{ah}), and resistance to the diffusion of vapor in large soil pores (r_{ss}). Time invariant terms include the psychrometric constant (γ) and the specific heat of air (C_p). β and α are time-varying wetness coefficients constrained between 0 and 1, where β scales potential evaporation down to actual evaporation, and α scales the saturated vapor pressure down to the actual vapor pressure at the soil surface. Briefly, r_{ss}, β, and α are determined using expressions derived from thermodynamics; all three terms depend on pedotransfer functions that rely on sand and clay fractions. We calculated these quantities using formulations from the literature, as done in Merlin et al. (2016); see the supporting information for details.

In summary, LE from equations (4) and (5) can be converted to soil E by dividing each LE term by the latent heat of vaporization (λ), converting from units of W/m^2 to mm/s. Thus, the daily soil evaporative flux is computed as:

$$E_d^{Soil} = \frac{86400}{\lambda}\left(w \cdot LE_d(r_{ss}, \alpha) + (1 - w) \cdot LE_d(\beta, \alpha)\right) \tag{6}$$

Where *w* is the unknown mixture weight; within the Bayesian framework, *w* is assigned a uniform prior, *w* ~ *Uniform*(0, 1). We used a temperature dependent λ, so that $\lambda = (2.501 - 0.00237 \cdot T_{\text{air}}) \cdot 10^6$, and 86400 converts seconds to days.

The DEPART framework treats certain soil property parameters as stochastic quantities to account for site-specific heterogeneity, accomplished by assigning these parameters relatively informative priors based on values expected to be representative of each site. We informed the variance of these stochastic quantities using the approximate standard deviation of field-based estimates calculated within each site. These parameters—which are excluded here but were used to calculate r_{ss}, β, and α—were the Clapp and Hornberger parameter, soil field capacity, residual soil moisture, soil moisture at saturation, and the parameterized air entry pressure. We allowed the von Karman constant, a constant for the logarithmic wind profile in the surface layer, to vary according to a uniform distribution on the interval (0.35, 0.42), consistent with past literature (Foken, 2006).

The DEPART framework models daily canopy intercepted E as:

$$E_d^{Intercepted} = \mathrm{P}_d(1 - exp(-k \cdot LAI_d)) \tag{7}$$

where P is the sum of same-day and previous-day precipitation, k is a decay parameter that is assigned a moderately informative prior based on a normal distribution with a moderate variance, $k \sim Normal(0.5, 10)$ (Li et al., 2019), and LAI is leaf area index. We estimated daily LAI using the Moderate Resolution Imaging Spectroradiometer (MODIS) leaf area index data product for AmeriFlux sites (ORNL DAAC, 2018). LAI from MODIS is only available every 8 days, so we linearly interpolated values to fill the gaps within each 8-day period. The total evaporative flux from leaf and soil surfaces in equation (1), E', is given as the sum of the soil evaporation term, E^{Soil} from equation (6), and intercepted evaporation, $E^{Intercepted}$ from equation (7).

This approach should provide more realistic estimates of daily E, reflecting the direct influence of rain events, and thus improve estimates of daily T and weekly WUE ($\mathrm{WUE}^{\mathrm{DEPART}}$). These shorter timescales (daily and weekly) should better capture the E, T, ET, and WUE responses to precipitation inputs in semiarid sites relative to the original (monthly scale) applications of the Scott and Biederman model. We ran this model in R (R Core Team, 2020) with the rjags package (Plummer, 2019) and the PostJAGS package (Fell, 2019) using Northern Arizona University's High Performance Computing resources.

2.6 Model Evaluation

To evaluate model fit, we compared R^2 values from a regression of DEPART predicted ET versus the observed ET for each site. To evaluate the contribution of T to ET, we also calculated T/ET values at annual timescales. Since T/ET is expected to be high in many ecosystem types (Wei et al., 2017), many studies use ET as a proxy for T (e.g., De Kauwe et al. [2019], Dralle et al. [2020], Emmerich [2007], Fisher et al. [2017]). However, a high T/ET does not necessarily mean T is highly correlated with ET, in which case using ET as a proxy for T would not be appropriate. Following this, to test whether T or E controls the pattern of ET, we also evaluated correlations between T and ET and between E and ET to assess if ET could be used as a suitable proxy for T at our study sites.

At the US-Mpj site only, we then compared T estimates from DEPART with T estimates from whole-tree sap flux from a previous study (Morillas et al., 2017) and to T estimates obtained from the Pérez-Priego et al. (2018) ET partitioning method. We only applied the Pérez-Priego et al. (2018) method at one site because it is fairly computationally intensive, and we picked US-Mpj to enable comparisons with sap flux data from Morillas et al. (2017). In this comparison, we considered correlations between sap flow T, Pérez-Priego T, and DEPART T, and the differences in how correlated T was to ET for each method over the time period in which all methods could be applied (2008-2012). Calculating the correlations between T estimates and comparing T/ET across methods helped us assess differences in the magnitude of T, while comparing correlations between T and ET helped us assess differences in the pattern of T compared to the bulk water flux.

Morillas et al. (2017) used 10 trees within the US-Mpj tower footprint to estimate T calculated from sap flow. Because the Morillas et al. (2017) study does not upscale T estimates to account for understory vegetation or the true boundaries of the tower footprint, we believe this T estimate to be only partially comparable to our own, and the magnitudes will likely differ. Still, the comparison could be useful when evaluating overall temporal patterns in T.

Like other popular ET partitioning methods (e.g., Table 1), the Pérez-Priego method makes assumptions about plant stomatal behavior that are not always well-suited to drylands. Therefore, the Pérez-Priego method may not be entirely reliable at the sites tested here, and this comparison should not be overvalued. We chose to compare our model to the Pérez-Priego

Table 3

Summary of DEPART model results across sites, including model fit (R^2), posterior means and 95% CIs for the average annual growing season T/ET and WUE values, and correlations (r) between T and E versus ET.

Gradient	Site	Model Fit (R^2)	T/ET	2.5% CI	97.5 % CI	WUE	2.5% CI	97.5 % CI	T vs. ET (*r*)	E vs. ET (*r*)
Low elevation, most arid	US-Seg	0.61	0.88	0.86	0.89	1.57	1.45	1.74	0.41	0.33
	US-Ses	0.51	0.84	0.82	0.85	1.37	1.25	1.48	0.22	0.30
Mid elevation	US-Wjs	0.70	0.94	0.93	0.94	2.02	1.96	2.09	0.61	0.17
	US-Mpj	0.63	0.87	0.73	0.90	2.40	2.07	7.37	0.51	0.18
High elevation, less arid	US-Vcp	0.81	0.96	0.95	0.96	2.74	2.65	2.83	0.74	0.07
	US-Vcm	0.83	0.88	0.84	0.91	1.05	0.99	1.12	0.71	0.08
	US-Vcs	0.91	0.96	0.95	0.97	2.11	1.97	2.25	0.72	0.05

Note. Here we define “annual growing season” as average values during spring, summer, and fall. Winter is excluded from these averages, since plants are inactive. R^2 values are computed using linear regressions. “CI” columns indicate credible intervals.

method, however, over other promising ET partitioning methods due to its simple-to-replicate documentation, and its thoroughness of incorporating optimality principles, which we are interested in testing here. Comparisons between T values were made using Spearman rank correlations to reduce the influence of outliers.

We also compared average monthly T/ET estimates from DEPART to monthly Scott and Biederman T/ET estimates for all NMEG sites, since the Scott and Biederman method was developed specifically for drylands where ET and GPP are tightly correlated.

2.7 Cross-wavelet Coherence Analysis

Application of the DEPART model to the daily ET and GPP data at each site results in predicted timeseries of weekly WUE^{DEPART} and daily T/ET. Using these timeseries, we analyzed the relationship between response variables WUE^{DEPART} and T/ET versus environmental variables (i.e., VPD, precipitation [P], SWC, and air temperature [T_{air}]) using cross-wavelet coherence analysis with a complex Morlet wavelet convolution (Grinsted et al., 2004; Torrence & Compo, 1998). Cross-wavelet coherence analysis allowed us to explore the relationship between variables across varying timescales by transforming a one-dimensional timeseries into two-dimensional time-frequency space. For example, we tested the weekly to yearly temporal coherence (R^2) between each response variable and multiple environmental variables, including lagged correlations, across all weeks in the timeseries. We then averaged the temporal coherences across all periods of time to summarize the correlations between the two variables as described in Samuels-Crow et al. (2018). To more intuitively represent in-phase (positively correlated) and anti-phase (negatively correlated) relationships, we modified the resulting R^2 values by multiplying R^2 values of anti-phase relationships by -1 to create a "temporal coherence index". This temporal coherence index can be either negative or positive; negative values represent anti-phase relationships and positive values represent in-phase relationships.

3 Results

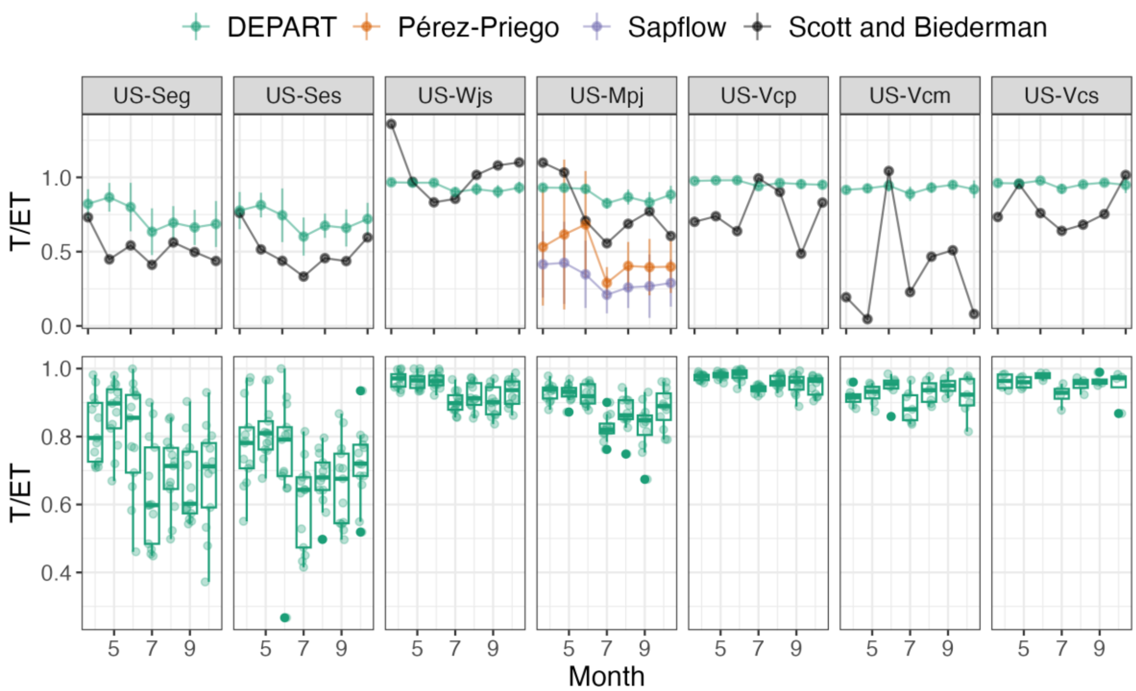

Figure 1. Comparison between average monthly T/ET (+/- standard deviation) using different partitioning methods (top panel). Pérez-Priego and sapflow derived T/ET (averaged over 2008-2012) are shown in the top panel for the US-Mpj site. DEPART T/ET and Scott and Biederman T/ET are averages over all available years of data for each site. When the Scott and Biederman T/ET is greater than 1, this indicates that the intercept in the ET versus GPP regression is negative, and the Scott and Biederman method may not be applicable. The bottom panel shows boxplots for all monthly DEPART T/ET estimates, where each overlayed point represents a monthly T/ET value.

3.1 Model Fit

The R^2 between daily estimated and observed ET varied from 0.51 to 0.81 across the elevation gradient (Table 3). Generally, the DEPART model performed better at the higher elevation, less arid sites than the lower elevation, more arid sites.

3.2 Comparison with Other ET Partitioning Methods

Excluding winter periods, and only including years that the DEPART model and the Pérez-Priego model could be compared to sapflow-based T estimates (2008-2012), the DEPART model estimated that T makes up the majority (90%) of ET at the US-Mpj site, but the Pérez-

Priego method estimated a much lower contribution (60%). The sapflow method resulted in the lowest contribution of T to ET (28%).

The correlation between the Pérez-Priego T estimates and the sapflow-based T estimates was slightly higher than the correlation between DEPART T estimates and the sapflow-based T estimates (r = 0.71 and r = 0.58, respectively). T estimates from DEPART and the Pérez-Priego model were also somewhat correlated with each other (r = 0.53) for the time periods both models could be applied (2008-2016).

The T estimates from DEPART were the most highly correlated with ET (r = 0.78) out of all three approaches, while the Pérez-Priego T estimates were the least correlated with ET (r = 0.41). The sapflow-based T estimates had an intermediate correlation with ET (r = 0.48).

After removing all days with rain events, T estimates from DEPART were more highly correlated with ET (r = 0.84 without rain events versus r = 0.78 with rain events). The same was true for the the Pérez-Priego T estimates (r = 0.49 versus r = 0.41) and sapflow-based T estimates (r = 0.55 versus r = 0.48). Additionally, during dry periods, T estimates from DEPART made up a larger fraction of ET (96% without rain events versus 90% with rain events), which also occurred for the Pérez-Priego T estimates (65% versus 60%) and sapflow-based T estimates (31% versus 28%). These results are consistent with the expectation that dryland ecosystems have greater T/ET during dry periods (and greater E/ET occurring on days with rain).

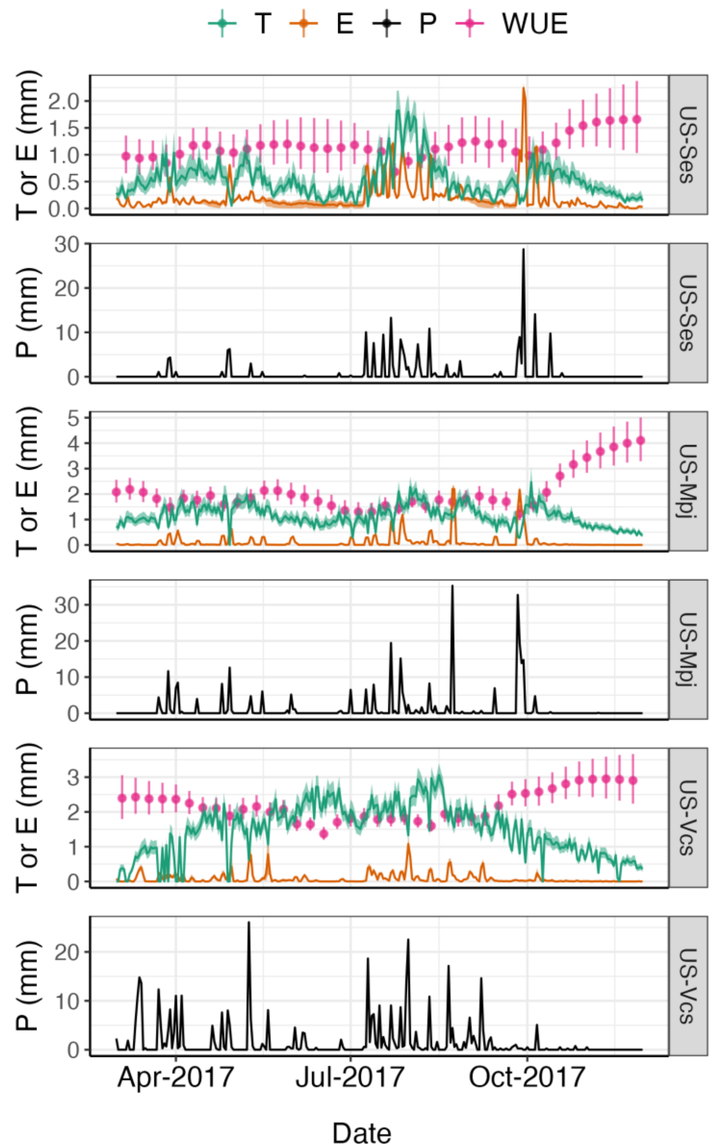

Figure 2. DEPART estimates of daily T and E fluxes and weekly WUE, along with observed daily P at representative low- (US-Ses), mid- (US-Mpj), and high-elevation (US-Vcs) sites during 2017. Symbols represent posterior means; error bars and shaded regions represent 95% credible intervals.

The comparison between monthly estimates of T/ET from DEPART and the Scott and Biederman approach showed that the latter agreed more with DEPART at lower elevation, more arid sites compared to higher elevation, less arid sites (Figure 1). The lower elevation, more arid sites also had more variable monthly T/ET. For sites associated with a relatively high R^2 from a regression of ET versus GPP (Figure S2), there is greater agreement between the DEPART and Scott and Biederman T/ET estimates. At the US-Mpj site, all ET partitioning methods are in disagreement.

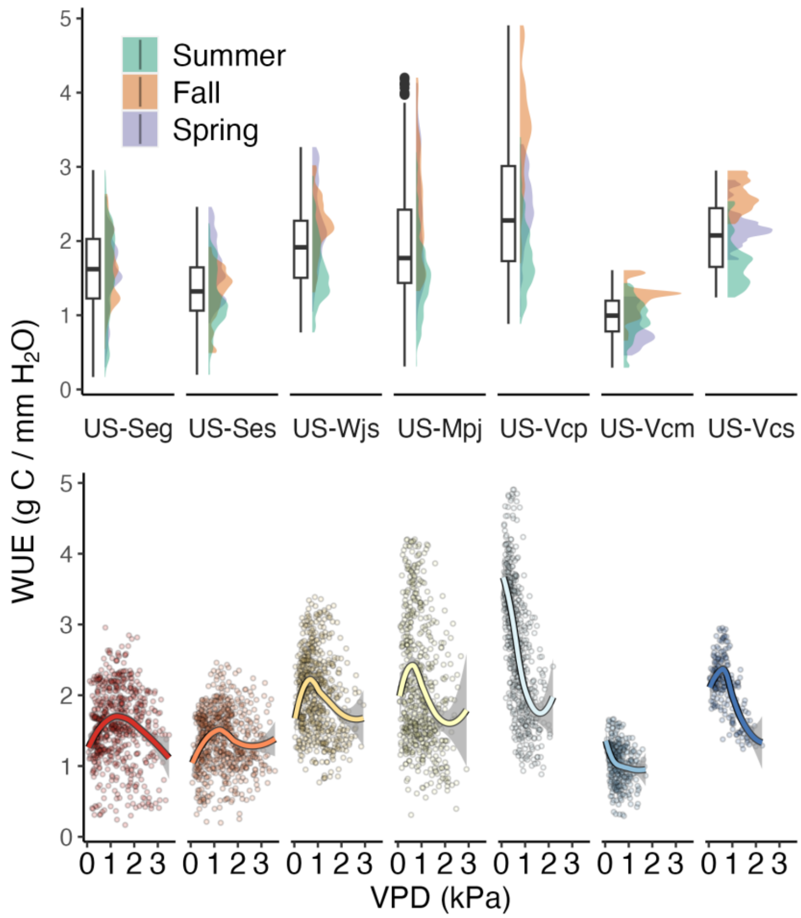

Figure 3. The top panel shows weekly WUE^{DEPART} estimated by the DEPART model. The WUE^{DEPART} presented here is an estimate of GPP/T. Large outliers occur outside of the growing season (early Spring and late Fall), when GPP and T are both very small. The bottom panel shows the relationship between WUE^{DEPART} and VPD by site.

3.3 Modeled T, E, and WUE Across Sites

The DEPART model suggests that T dominated ET across the aridity gradient (annual growing season T/ET generally ranged from 0.75 to 0.93), and T and E became temporally staggered around episodic precipitation events in which E peaks faster than T (Figure 2), which is consistent with previous dryland ET partitioning studies (Sun et al., 2019). Regardless of the overall contribution of T to ET at each site, E was more correlated with ET at lower elevation, more arid sites, and T was more correlated with ET at higher elevation, less arid sites (Table 2).

Annual growing season WUE^{DEPART} ranged from 0.97 to 2.44 g C/mm H_2O across sites and years, although WUE^{DEPART} generally showed a more distinct separation across seasons (spring, summer, and fall) at the higher elevation, less arid sites compared to the lower elevation, more arid sites (Figure 3).

3.4 Cross-wavelet Coherence Analysis

In general, the cross-wavelet coherence results show that the lower elevation, more arid sites are supply-driven and the higher elevation, less arid sites are demand-driven. For example, VPD and temperature (important at high elevation sites) influence the magnitude of

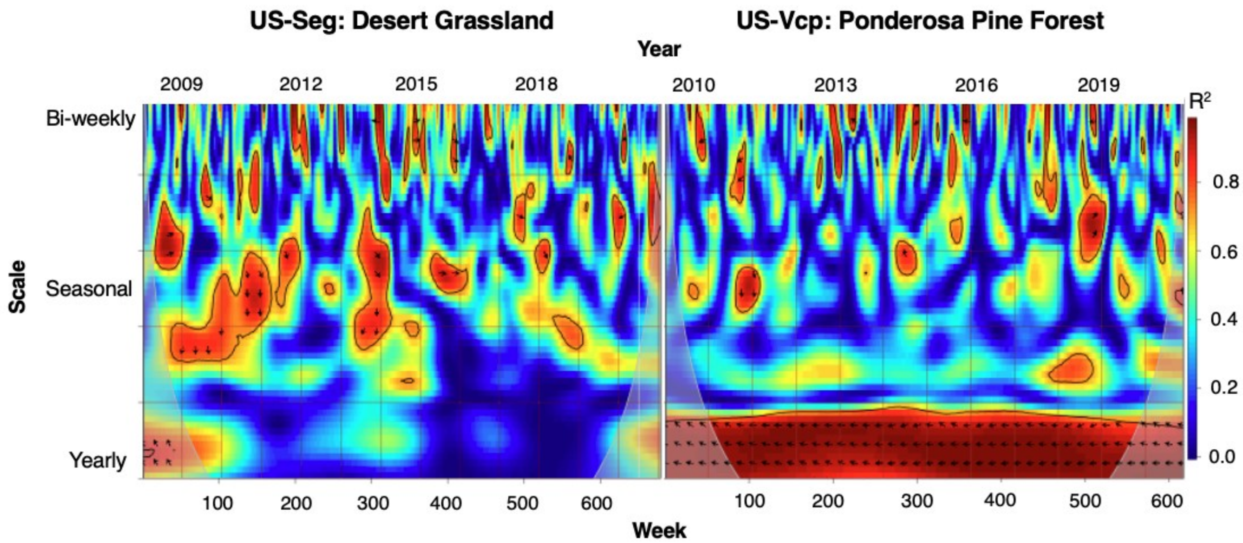

Figure 4. Cross-wavelet coherence plots for weekly WUE^{DEPART} versus VPD at the desert grassland site (US-Seg) (left) and ponderosa pine site (US-Vcp) (right). The colors represent the temporal coherence (R^2). Warmer colors represent time periods when there is significant interrelation between WUE^{DEPART} and VPD. Colder colors represent time periods when there is less dependence between WUE^{DEPART} and VPD. Arrow direction represents whether a variable is leading or lagging. Arrows point to the right when the timeseries are in phase (the variables move in the same direction) and to the left when they are anti-phase (the variables move in opposite directions). Arrows pointing to the right-down or left-up indicate that VPD is leading, while arrows pointing to the right-up or left-down indicate that WUE^{DEPART} is leading.

atmospheric demand for moisture whereas soil moisture (important at low elevation sites) influences the magnitude of moisture supply (Grossiord et al., 2020).

The cross-wavelet coherence also showed that the relationship between WUE^{DEPART} and VPD (Figure 4 and Figure 5) varied across sites and timescales. At the less arid sites, WUE^{DEPART} and VPD were consistently in-phase (i.e., positively correlated) at the yearly timescale, but WUE^{DEPART} and VPD were only occasionally correlated at the sub-monthly timescale. In contrast, WUE^{DEPART} and VPD were anti-phase (i.e., negatively correlated) at the yearly timescale at the woody plant-dominated low- and mid-elevation sites. The lowest elevation site (US-Seg, desert grassland) did not support a strong relationship between WUE^{DEPART} and VPD at the yearly timescale, although there was sometimes a strong anti-phase relationship at the seasonal timescale.

In general, we found that WUE^{DEPART} at higher elevation, less arid sites was more consistently correlated with environmental variables associated with the atmospheric demand for moisture (e.g., VPD, T_{air}) at yearly timescales. At lower elevation, more arid sites, WUE^{DEPART} was more consistently correlated with indices of water availability (e.g., SWC, P) at weekly and seasonal timescales (Figure 5; Figure S3). At the lower elevation sites, WUE^{DEPART} and SWC had a strong relationship and were generally in-phase at the monthly to yearly timescales (Figure 5). The same was true for WUE^{DEPART} and P at the lower elevation sites, but the relationship between WUE^{DEPART} and P was also anti-phase at sub-monthly timescales.

According to the cross-wavelet coherence results for T/ET versus key environmental variables (see Figure 5 and Figure S3), T/ET had the strongest relationships with variables indicating the availability of water (e.g., SWC, P), and weaker relationships with variables associated with the atmospheric demand for moisture and seasonality (e.g., VPD and T_{air}). The weak relationship between T/ET versus VPD and T_{air} is likely because T and E are correlated with these drivers on similar timescales, and so T/ET appears independent of these drivers. However, the combination of in-phase and anti-phase relationships between T/ET versus SWC and P show that T and ET respond to the presence of water on distinct timescales. For example, T/ET and P are typically anti-phase at daily to monthly timescales and in-phase at seasonal timescales (Figure 5; Figure S3), likely due to high E after large water pulses during episodic rain events. In other words, E is more strongly controlled by P compared to T at daily timescales, but T is more strongly controlled by P compared to E at seasonal to yearly timescales. In contrast, T/ET and SWC are mostly in-phase across daily to seasonal timescales. However, the T/ET versus SWC relationship becomes anti-phase at yearly timescales at the more arid sites, showing a juxtaposition between the timescales over which P or SWC are related to T/ET.

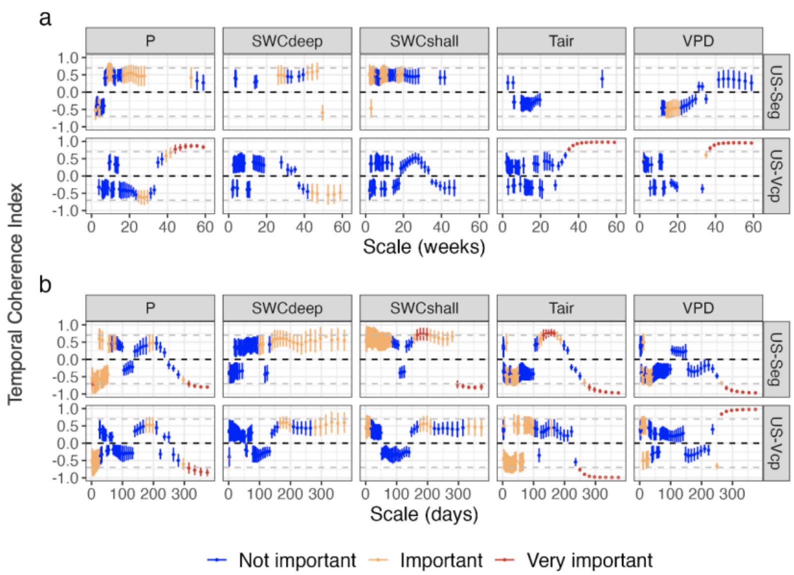

Figure 5. A summary of the cross-wavelet coherence results for (a) WUE and (b) T/ET versus multiple environmental variables at the desert grassland site (US-Seg) and ponderosa pine site (US-Vcp). Plots show the average temporal coherence index values (y-axis) across the entire timeseries for each temporal scale (x-axis). This is essentially taking the horizontal average of the values in the graphs shown in Figure 4 for every temporal scale, but only includes the time periods when WUE or T/ET are lagging. Note that here, the temporal coherence index is a modified temporal coherence where positive values indicate the series are in phase (equivalent to arrows pointing right in Figure 4) and negative values mean the series are anti-phase (arrows pointing left in Figure 4). The whiskers indicate the standard deviation of temporal coherence index values. The colors correspond to the temporal coherence, such that blue represents less dependence between WUE^{DEPART} or T/ET and environmental variables. Values over 0.7 or under -0.7 (gray dashed lines) correspond to strong temporal coherence.

4 Discussion

To overcome the challenges of previous ET partitioning methods, we built a novel ET partitioning approach to produce estimates of daily E and T and weekly WUE^{DEPART} across semiarid ecosystem types. We then used these estimates to evaluate the spatiotemporal variability in T/ET and WUE^{DEPART}, and to determine the relationships between T/ET and WUE^{DEPART} versus environmental variables across timescales.

4.1 T/ET and WUE Across Sites

The contribution of T to ET has been controversial in semiarid ecosystems, and T/ET estimates from previous synthesis studies have varied depending on the method used (Sun et al., 2019; Wei et al., 2017). Here, we found high T/ET across an aridity gradient in the southwestern USA (Table 3). However, there was notable year-to-year variability in monthly T/ET at the two driest sites, which is consistent with previous dryland literature (Reynolds et al., 2000). Generally, after an episodic precipitation event, E increased immediately and peaked quickly, whereas T increased and peaked more slowly, likely due to lags associated with plant water uptake (Gardner, 1991; Kramer, 1938). Because of these lags, E can still reach or surpass T during certain times of the growing season at the more arid sites (Cavanaugh et al., 2011; Scott et al., 2006) (Figure 2).

The high T/ET values estimated by DEPART are quite different from previous studies that have found values generally spanning 40-70% in drylands (Cavanaugh et al., 2011; Nelson et al., 2020; Pérez-Priego et al., 2018; Scott et al., 2006, 2021; Scott & Biederman, 2017). However, previous meta-analyses have found inconsistent T/ET estimates across ecosystem types (Miralles et al., 2011; Sun et al., 2019; Wei et al., 2017). The high T/ET in this study aligns most closely with catchment-scale isotopic ET partitioning studies (Jasechko et al., 2013) but not with stand-level sapflow studies, which typically estimate lower T/ET compared to isotopic studies (Schlesinger & Jasechko, 2014). While there are biases to consider in all ET partitioning approaches, sapflow-based stand-level studies could be underestimating T/ET because they often neglect understory vegetation and assume the dynamics of the instrumented plants represent a larger area. At the same time, isotope-based studies may yield biased estimates of T/ET when hydrologic decoupling is a concern (Brooks, Renée et al., 2010; Schlesinger & Jasechko, 2014). It is worth noting that T/ET averages reported in synthesis studies are frequently composed of estimates from different methodologies with different assumptions.

In support of high T/ET in semiarid ecosystems, consider Figure 6. In 2011 at the US-Mpj site, from the beginning of April until the end of June, there were almost no precipitation inputs and shallow SWC remained very low. Figure 6 shows that the higher-than-average DEPART T/ET estimates hover near 100%, while the sapflow-based estimates from a previous study oscillate around 50%. In this deep-rooted piñon-juniper ecosystem at the end of June, following three months of almost no precipitation, how could 50% of ET be attributed to soil evaporation, E? A large contribution of T (e.g., T/ET close to 1) would seem reasonable in this scenario, which is likely associated with exceptionally dry surface soils, where little / no water is available for direct evaporation, but trees likely have access to deeper water sources protected from evaporation. High dryland T/ET is also consistent with the idea that a dry shallow soil surface can act as a boundary layer that prevents further evaporation from occurring (Yamanaka & Yonetani, 1999). It follows that ET from drylands can have high T/ET, except immediately following rain events that result in moist surface soils. At the same time, the high DEPART T/ET (Figure 6) values that closely follow precipitation inputs are likely overestimated around rain events, as modeled E may be decreasing too rapidly after a rain event. Other studies have shown that E may decrease after precipitation inputs according to a decay function and at a rate that varies with soil textural properties (Li et al., 2019). Considering this, further improvements on the physical E models (such as those included in Lehmann et al., 2018 or Or et al., 2013) likely could improve DEPART estimates.

Eddy flux towers do not provide direct measurement of T or E, which makes it challenging to assess the performance of flux tower-based ET partitioning models (Stoy et al., 2019). However, in Table 1 we highlighted why other flux tower-based ET partitioning approaches may not be best suited for semiarid ecosystems, such as our study sites. Briefly, many flux tower-based ET partitioning methods (including both data-driven and process-based methods) may underestimate T in semiarid ecosystems by overestimating WUE. Many of these methods consider estimating WUE to be the primary barrier to estimating T. However, it is more accurate to consider this problem circular, as we are attempting for solve for two unknowns (i.e., WUE and T). For instance, as a community we want to partition ET using an estimate of WUE (GPP/T) along with some estimate of GPP from NPP partitioning approaches. At the same time, it is difficult to estimate GPP/T without partitioning ET. Many ET partitioning methods (Nelson et al., 2018; Pérez-Priego et al., 2018; Zhou et al., 2016) get around this by calculating T and GPP/T simultaneously by assuming GPP/ET = GPP/T during dry periods to estimate transpirational WUE (GPP/T) for all (both wet and dry) periods. This assumption likely introduces biases into the WUE and T calculations, as past studies have shown that various WUE indices are expected to be lower during wet periods compared to dry periods in semiarid ecosystems, including transpirational WUE (Donovan & Ehleringer, 1992), intrinsic WUE (Lázaro-Nogal et al., 2015), and ecosystem WUE (Guoju et al., 2013; Tarin et al., 2020). Note that overestimating WUE (GPP/T) forces T in the denominator to be lower, so it follows that a higher WUE is equivalent to lower T and lower T/ET estimates. By ignoring wet periods, the Pérez-Priego method and others may overestimate true transpirational WUE when dryland plants are stimulated by precipitation pulses. DEPART, which does not ignore rainy periods, produces higher T/ET estimates compared to the Pérez-Priego method and others (Nelson et al., 2020).

DEPART represents a departure from the assumption that WUE is constant across rainy and dry periods, and is perhaps more applicable to ecosystems with dynamic WUE.

The DEPART results also show variability in WUE^{DEPART} between wet and dry periods, although there was greater seasonal variation in estimated WUE^{DEPART} at the tree-dominated sites (US-Wjs, US-Mpj, US-Vcp, and US-Vcs) than the shrub- and grass-dominated sites (US-Seg, US-Ses, and US-Vcm) (Figure 3). Regardless, WUE^{DEPART} was generally lowest during the middle of the growing season around precipitation pulses (Figure 2). This further supports that ET partitioning methods that calculate WUE based on periods without precipitation (Nelson et al., 2018; Pérez-Priego et al., 2018; Zhou et al., 2016) or that even assume WUE is constant (Scott & Biederman, 2017; Zhou et al., 2016) should be used with caution in ecosystems that are heavily influenced by episodic precipitation pulses.

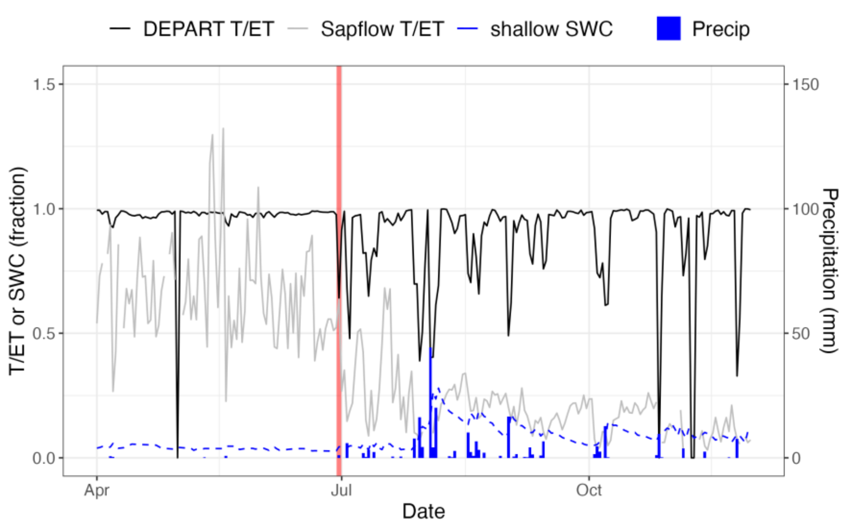

Figure 6. An example of DEPART T/ET (black line) and sapflow T/ET (gray line) at US-Mpj during a dry growing season (2011). The red vertical line indicates the onset of the monsoon rainy season. From April until the end of June, there is almost no precipitation (blue bars) and shallow SWC (dashed blue line) is very low.

Regardless of the overall contribution of T to ET at each site, E was more strongly correlated with ET at lower elevation, more arid sites, while T was more strongly correlated with ET at higher elevation, less arid sites (Table 3). This has implications for studies that use ET as a proxy for T in drylands: even if T makes up a majority of ET at a particular site, temporal changes (patterns) in ET could be more indicative of changes in E rather than changes in T (such as at the shrubland site, US-Ses; Table 3). For example, studies that use ET as a proxy for T to test the relationship between plant water-use and environmental variables (De Kauwe et al., 2019; Kropp et al., 2017) may be testing something closer to the relationship between abiotic water flux patterns (e.g., E) and environmental variables. In other words, E can control the variability in ET even when T makes up the majority in ET, so partitioning ET is still useful even when T is high.

4.2 Temporal Scale, WUE, and T/ET

Different conclusions about how environmental drivers affect plant water-use across different scales are not necessarily contradictory. Rather, these conclusions are representative of how spatial and temporal scale affect plant observations (Jarvis & McNaughton, 1986). Here we demonstrate the importance of observing WUE^{DEPART} and T/ET dynamics over varying temporal scales. Specifically, the cross-wavelet coherence results indicate that temporal coherence between WUE^{DEPART} and T/ET and different potential drivers depends on the temporal scale the relationship is observed over. Previous studies have found inconsistent results with regards to the influence of VPD versus SWC on plant water dynamics (Kwon et al., 2018; Lévesque et al., 2014; Schultz & Stoll, 2010), and the effects of VPD and SWC on T can be difficult to disentangle (Novick et al., 2016). The temporal coherences in our study suggest that the lower elevation, more arid sites are more limited by shallow SWC (supply driven), and higher elevation sites are more limited by VPD (demand driven). However, at the more arid sites this coupling occurred at shorter timescales compared to the less arid sites (Figure 5). At the less arid sites (where VPD was often important), deep SWC was also sometimes important over longer timescales, likely due to the role of deep roots in these taller statured ecosystems (Novick et al., 2016). Following this, seemingly contradictory results about the potential influence of VPD versus SWC on plant water dynamics could be due to temporal variations in ecosystem-specific processes.

Temporal scale is also important for understanding the relationship between T/ET and environmental variables. For example, previous studies found a low correlation between T/ET and potentially important environmental variables across ecosystem types (Nelson et al., 2020; Sun et al., 2019). We also found that T/ET had low temporal coherence with many environmental variables, or inconsistent relationships with those variables over different timescales. This low temporal coherence is likely because T and E share similar environmental drivers, so the ratio T/ET does not change much despite potentially large changes in T and E. However, although T and E respond to similar drivers, they respond to those drivers over varying timescales. Specifically, T responds more slowly than E to changes in water supply (Kerhoulas et al., 2013), so there was higher coherence between T/ET and water supply-associated variables (i.e., P and SWC) across longer timescales.

The temporal coherence between WUE^{DEPART} and potential environmental drivers is generally consistent with past literature focused on intrinsic WUE (Grossiord et al., 2020), but is not consistent with literature representing ecosystem WUE calculated as GPP/ET (Stoy et al., 2019). This supports the idea that WUE^{DEPART} is representative of biological WUE at the ecosystem scale with less dilution from abiotic variables such as E. For example, it is known that the relationship between intrinsic WUE and VPD is nonlinear; i.e., WUE increases with VPD up to a point but decreases thereafter, for very high values of VPD (Zhang et al., 2019). Using the NMEG's natural aridity gradient, the WUE^{DEPART} cross-wavelet coherence results show this hyperbolic pattern (e.g., WUE^{DEPART} and VPD have a positive relationship at less arid sites but a negative relationship at more arid sites). This nonlinear relationship is also true within sites at the weekly timescale over the entire study period (Figure 3), with the exception of two high elevation sites (US-Vcp and US-Vcm) that more closely match the relationship found for GPP/ET and VPD in Stoy et al. (2019), although this could be due to the smaller range of VPD experienced at those sites.

Besides VPD, WUE^{DEPART} is likely controlled by multiple other environmental drivers, and the relationship between WUE and these drivers likely depends on plant functional type (Grossiord et al., 2020). For example, it is known that soil moisture can modulate the relationship between WUE and VPD (Novick et al., 2016), depending on plant physiological strategy (Ambika & Mishra, 2021; W. Zhang et al., 2023). The inconsistent relationship between WUE^{DEPART} and VPD at the sub-yearly timescale (Figure 4 and Figure 5) suggests that implementing assumptions of stomatal optimality—which result in assuming strong coupling of WUE and VPD—may be inappropriate for partitioning ET in semiarid ecosystems at certain timescales. Only considering the effects of VPD on WUE could be especially inappropriate in more arid ecosystems such as the desert grassland (US-Seg) and shrubland (US-Ses) studied here, where SWC is more frequently important than VPD. This study shows that the patterns between WUE and environmental variables are inconsistent within sites, and future research should aim to determine the conditions under which biological WUE (such as WUE^{DEPART}) exhibits expected (e.g., optimal) and unexpected behavior at the ecosystem scale.

Many previous ET partitioning methods are tied to assumptions of optimality that only consider VPD. The cross-wavelet coherence results show that the timescales of optimality (e.g., for responses of WUE^{DEPART} and T/ET to VPD) in drylands may not be consistent or intuitive, and thus model applications that use optimality theory should be used with caution. WUE^{DEPART} and T/ET had high temporal coherence with other variables that influence the magnitude of moisture supply, such as SWC and P, so WUE^{DEPART} and T/ET patterns are likely controlled by site-dependent environmental variables. For example, at the more arid sites, WUE^{DEPART} is likely more strongly tied to P and SWC due to growing season rain pulse dynamics (Feldman et al., 2021; Loik et al., 2004). In contrast, the less arid, higher elevation sites contain more plant species known to be isohydric (Anderson-Teixeira et al., 2011; Samuels-Crow et al., 2020), such as *Pinus ponderosa* (at the US-Vcp site), and we might expect T and WUE to be more tightly coupled to VPD at these sites.

It is worth noting that WUE links plant water loss to plant carbon uptake, the latter of which can also change in response to environmental conditions (Ehleringer & Cerling, 1995). Historically, the effects of VPD on WUE are explained by the effects of VPD on the intercellular CO_2 concentration (C_i). Because the effects of VPD on C_i were found to be similar to the effects of VPD on stomatal conductance, it has become common to lump these two processes together when evaluating the effects of environmental variables on WUE (Grossiord et al., 2020). However, stomatal conductance has a wide variety of responses to environmental variables depending on plant strategy. For example, abscisic acid mediates stomatal conductance in response to low SWC, and can complicate stomatal responsiveness to VPD (Kriedemann et al., 1972; Rogiers et al., 2012). It could be that at more arid sites, the differences in WUE^{DEPART} patterns are indicative of a divergence of leaf-derived C_i responses to VPD and root-driven stomatal responses to low SWC. In other words, stomata in more arid ecosystems can exhibit more anisohydric behaviors in response to VPD but could still respond to abscisic acid.

4.3 ET Partitioning Model Limitations

Because the ET partitioning methods developed thus far are not in consensus, it is beneficial to explore the underlying assumptions of each model to determine which ET partitioning method is best suited to a particular site (Table 1). As a semi-mechanistic framework, DEPART represents an alternative to previous process-based ET partitioning methods that make assumptions about plant water-use traits (Pérez-Priego et al., 2018) and more data-driven, empirical approaches (Nelson et al., 2018). However, the process-based component of DEPART is abiotic in its assumptions (i.e., the soil evaporation equations). Because we are allowing certain parameters in these abiotic equations to vary stochastically, we intend to allow sufficient flexibility in these parameters to account for the inaccuracies of the specific process-based formulation or limitations of field data used to inform parameters in the equations. For example, DEPART is limited by the availability of SWC data and knowledge of soil textural properties. While SWC data are typically available as a flux tower site data product, knowledge of sand and clay fractions is less common. However, soil textural properties can also be sourced from global data products such as SoilGrids2.0 (Poggio et al., 2021). Still, the process-based evaporation equations likely do not capture the full heterogeneity of the flux tower footprint, and do not account for variables such as vegetation cover. Merlin et al. (2016) found that a soil evaporation model, similar to the models used in DEPART, produced E estimates that were moderately correlated with observed E (average $R^2 = 0.57$) for sites with percent clay that align with the percent clay ranges measured at our study sites. Therefore, DEPART would likely benefit from the inclusion of better performing evaporation models and there is likely more room for improvement in constraining evaporation to partition ET.

5 Conclusion

This study presents a fine-scale ET partitioning framework suitable for future application in water-limited ecosystems with flashy E/ET dynamics, which has rarely been addressed in past ET partitioning literature. The results obtained from the DEPART framework improved our understanding of the contribution of T and E to ET in semiarid ecosystems by revealing the timescales at which T/ET and WUE^{DEPART} have significant relationships with environmental variables. By estimating intrinsic WUE^{DEPART} at the ecosystem scale, along a semiarid aridity gradient, we found that WUE^{DEPART} is driven by moisture supply in more arid ecosystems and moisture demand in less arid ecosystems. DEPART is a reproducible ET partitioning method that can be applied at many flux tower sites. Thus, this study complements a suite of recent ET partitioning studies by introducing a new approach that can be applied to drylands.

Acknowledgments

This research was supported by NSF Hydrologic Sciences award EAR1834699 to K.S-C., K.O., and M.L., a DOE Ameriflux Management Project award to M.L., a USGS-NSF Internship Program supplement to award EAR1834699, a NASA FINESST award 80NSSC22K1443 to E.R. and K.O., and the Interns-to-Scholars program at Northern Arizona University. We would also like to thank Bilal Aslam and Andrew Richardson for providing significant manuscript feedback, Michael Fell for his R functions for summarizing Bayesian output, and Selena Pearson and Portia Irey for assisting with the soil texture lab analyses. Any use of trade, firm, or product names is for descriptive purposes only and does not imply endorsement by the U.S. Government.

Open Research

All code, models, and data files for the gap-filled flux tower site data, soil texture data, and model output used for the analyses in this paper can be found on Zenodo (Reich et al., 2023a). Code and models can also be found in the Github repository and on Zenodo: https://github.com/egreich/A-semi-mechanistic-model-for-partitioning-evapotranspiration (Reich et al., 2023b).

References

Ambika, A. K., & Mishra, V. (2021). Modulation of Compound Extremes of Low Soil Moisture and High Vapor Pressure Deficit by Irrigation in India. *Journal of Geophysical Research: Atmospheres*, *126*(7), e2021JD034529. https://doi.org/10.1029/2021JD034529

Anderson-Teixeira, K. J., Delong, J. P., Fox, A. M., Brese, D. A., & Litvak, M. E. (2011). Differential responses of production and respiration to temperature and moisture drive the carbon balance across a climatic gradient in New Mexico: CARBON BALANCE ACROSS NM ELEVATIONAL GRADIENT. *Global Change Biology*, *17*(1), 410–424. https://doi.org/10.1111/j.1365-2486.2010.02269.x

Baldocchi, D. (2014). Measuring fluxes of trace gases and energy between ecosystems and the atmosphere – the state and future of the eddy covariance method. *Global Change Biology*, *20*(12), 3600–3609. https://doi.org/10.1111/gcb.12649

Baldocchi, D. (2020). How eddy covariance flux measurements have contributed to our understanding of Global Change Biology. *Global Change Biology*, *26*(1), 242–260. https://doi.org/10.1111/gcb.14807

Baldocchi, D., FAlge, Ev., Gu, L., Olson, R., & al, et. (2001). FLUXNET: A new tool to study the temporal and spatial variability of ecosystem-scale carbon dioxide, water vapor, and energy flux densities. *Bulletin of the American Meteorological Society*, *82*(11), 2415–2434.

Beer, C., Ciais, P., Reichstein, M., Baldocchi, D., Law, B. E., Papale, D., et al. (2009). Temporal and among-site variability of inherent water use efficiency at the ecosystem level. *Global Biogeochemical Cycles*, *23*(2). https://doi.org/10.1029/2008GB003233

Bradford, J. B., & Lauenroth, W. K. (2006). Controls over invasion of Bromus tectorum: The importance of climate, soil, disturbance and seed availability. *Journal of Vegetation Science*, *17*(6), 693–704. https://doi.org/10.1111/j.1654-1103.2006.tb02493.x

Bradford, J. B., Schlaepfer, D. R., Lauenroth, W. K., & Burke, I. C. (2014). Shifts in plant functional types have time-dependent and regionally variable impacts on dryland ecosystem water balance. *Journal of Ecology*, *102*(6), 1408–1418. https://doi.org/10.1111/1365-2745.12289

Bradford, J. B., Schlaepfer, D. R., Lauenroth, W. K., & Palmquist, K. A. (2020). Robust ecological drought projections for drylands in the 21st century. *Global Change Biology*, *26*(7), 3906–3919. https://doi.org/10.1111/gcb.15075

Brooks, Renée, J., Barnard, H. R., Coulombe, R., & McDonnell, J. J. (2010). Ecohydrologic separation of water between trees and streams in a Mediterranean climate. *Nature Geoscience*, *3*(2), 100–104. https://doi.org/10.1038/ngeo722

Cavanaugh, M. L., Kurc, S. A., & Scott, R. L. (2011). Evapotranspiration partitioning in semiarid shrubland ecosystems: a two-site evaluation of soil moisture control on transpiration. *Ecohydrology*, *4*(5), 671–681. https://doi.org/10.1002/eco.157

Daac, O. (2017). MODIS and VIIRS Land Products Fixed Sites Subsetting and Visualization Tool. *ORNL DAAC*. https://doi.org/10.3334/ORNLDAAC/1567

De Kauwe, M. G., Medlyn, B. E., Pitman, A. J., Drake, J. E., Ukkola, A., Griebel, A., et al. (2019). Examining the evidence for decoupling between photosynthesis and transpiration during heat extremes. *Biogeosciences*, *16*(4), 903–916. https://doi.org/10.5194/bg-16-903-2019

Desai, A. R., Richardson, A. D., Moffat, A. M., Kattge, J., Hollinger, D. Y., Barr, A., et al. (2008). Cross-site evaluation of eddy covariance GPP and RE decomposition techniques. *Agricultural and Forest Meteorology*, *148*(6), 821–838. https://doi.org/10.1016/j.agrformet.2007.11.012

Dong, N., Prentice, I. C., Wright, I. J., Evans, B. J., Togashi, H. F., Caddy-Retalic, S., et al. (2020). Components of leaf-trait variation along environmental gradients. *New Phytologist*, *228*(1), 82–94. https://doi.org/10.1111/nph.16558

Donovan, L. A., & Ehleringer, J. R. (1992). Contrasting Water-Use Patterns Among Size and Life-History Classes of a Semi-Arid Shrub. *Functional Ecology*, *6*(4), 482–488. https://doi.org/10.2307/2389287

Dralle, D. N., Hahm, W. J., Rempe, D. M., Karst, N., Anderegg, L. D. L., Thompson, S. E., et al. (2020). Plants as sensors: vegetation response to rainfall predicts root-zone water storage capacity in Mediterranean-type climates. *Environmental Research Letters*, *15*(10), 104074. https://doi.org/10.1088/1748-9326/abb10b

Ehleringer, J. R., & Cerling, T. E. (1995). Atmospheric CO2 and the ratio of intercellular to ambient CO2 concentrations in plants. *Tree Physiology*, *15*(2), 105–111. https://doi.org/10.1093/treephys/15.2.105

Eichelmann, E., Mantoani, M. C., Chamberlain, S. D., Hemes, K. S., Oikawa, P. Y., Szutu, D., et al. (2022). A novel approach to partitioning evapotranspiration into evaporation and transpiration in flooded ecosystems. *Global Change Biology*, *28*(3). https://doi.org/10.1111/gcb.15974

Emmerich, W. E. (2007). Ecosystem Water Use Efficiency in a Semiarid Shrubland and Grassland Community. *Rangeland Ecology & Management / Journal of Range Management Archives*, *60*(5), 464–470.

Engelbrecht, B. M. J., Comita, L. S., Condit, R., Kursar, T. A., Tyree, M. T., Turner, B. L., & Hubbell, S. P. (2007). Drought sensitivity shapes species distribution patterns in tropical forests. *Nature*, *447*(7140), 80–82. https://doi.org/10.1038/nature05747

Feldman, A. F., Chulakadabba, A., Gianotti, D. J. S., & Entekhabi, D. (2021). Landscape-Scale Plant Water Content and Carbon Flux Behavior Following Moisture Pulses: From Dryland to Mesic Environments. *Water Resources Research*, *57*(1), e2020WR027592. https://doi.org/10.1029/2020WR027592

Fell, M. (2019). PostJAGS. R. Retrieved from https://github.com/fellmk/PostJAGS (Original work published September 12, 2018)

Feng, X., Lu, Y., Jiang, M., Katul, G., Manzoni, S., Mrad, A., & Vico, G. (2022). Instantaneous stomatal optimization results in suboptimal carbon gain due to legacy effects. *Plant, Cell & Environment*, *45*(11), 3189–3204. https://doi.org/10.1111/pce.14427

Fisher, J. B., Melton, F., Middleton, E., Hain, C., Anderson, M., Allen, R., et al. (2017). The future of evapotranspiration: Global requirements for ecosystem functioning, carbon and climate feedbacks, agricultural management, and water resources. *Water Resources Research*, *53*(4), 2618–2626. https://doi.org/10.1002/2016WR020175

Foken, T. (2006). 50 Years of the Monin–Obukhov Similarity Theory. *Boundary-Layer Meteorology*, *119*(3), 431–447. https://doi.org/10.1007/s10546-006-9048-6

Gan, G., & Liu, Y. (2020). Inferring transpiration from evapotranspiration: A transpiration indicator using the Priestley-Taylor coefficient of wet environment. *Ecological Indicators*, *110*, 105853. https://doi.org/10.1016/j.ecolind.2019.105853

Garcia Coronado, J., Medina Gonzalez, H., & Nunnez Acosta, D. (2008). Hydrometer method: influence of the times of readings in the determination of the size distribution of particles in soil of Havana. Retrieved from https://www.osti.gov/etdeweb/biblio/22244942

Gardner, W. R. (1991). Modeling water uptake by roots. *Irrigation Science*, *12*(3), 109–114. https://doi.org/10.1007/BF00192281

Gomarasca, U., Migliavacca, M., Kattge, J., Nelson, J. A., Niinemets, Ü., Wirth, C., et al. (2023). Leaf-level coordination principles propagate to the ecosystem scale. *Nature Communications*, *14*(1), 3948. https://doi.org/10.1038/s41467-023-39572-5

Grinsted, A., Moore, J. C., & Jevrejeva, S. (2004). Application of the cross wavelet transform and wavelet coherence to geophysical time series. *Nonlinear Processes in Geophysics*, *11*(5/6), 561–566. https://doi.org/10.5194/npg-11-561-2004

Grossiord, C., Buckley, T. N., Cernusak, L. A., Novick, K. A., Poulter, B., Siegwolf, R. T. W., et al. (2020). Plant responses to rising vapor pressure deficit. *New Phytologist*, *226*(6), 1550–1566. https://doi.org/10.1111/nph.16485

Guo, J. S., Hultine, K. R., Koch, G. W., Kropp, H., & Ogle, K. (2020). Temporal shifts in iso/anisohydry revealed from daily observations of plant water potential in a dominant desert shrub. *New Phytologist*, *225*(2), 713–726. https://doi.org/10.1111/nph.16196

Guoju, X., Fengju, Z., Zhengji, Q., Yubi, Y., Runyuan, W., & Juying, H. (2013). Response to climate change for potato water use efficiency in semi-arid areas of China. *Agricultural Water Management*, *127*, 119–123. https://doi.org/10.1016/j.agwat.2013.06.004

Jarvis, P. G., & McNaughton, K. G. (1986). Stomatal Control of Transpiration: Scaling Up from Leaf to Region. In A. MacFadyen & E. D. Ford (Eds.), *Advances in Ecological Research* (Vol. 15, pp. 1–49). Academic Press. https://doi.org/10.1016/S0065-2504(08)60119-1

Jasechko, S., Sharp, Z. D., Gibson, J. J., Birks, S. J., Yi, Y., & Fawcett, P. J. (2013). Terrestrial water fluxes dominated by transpiration. *Nature*, *496*(7445), 347–350. https://doi.org/10.1038/nature11983

Kerhoulas, L. P., Kolb, T. E., & Koch, G. W. (2013). Tree size, stand density, and the source of water used across seasons by ponderosa pine in northern Arizona. *Forest Ecology and Management*, *289*, 425–433. https://doi.org/10.1016/j.foreco.2012.10.036

Komatsu, T. S. (2003). Toward a Robust Phenomenological Expression of Evaporation Efficiency for Unsaturated Soil Surfaces. *Journal of Applied Meteorology*, *42*(9), 1330–1334. https://doi.org/10.1175/1520-0450(2003)042<1330:TARPEO>2.0.CO;2

Kramer, P. J. (1938). Root Resistance as a Cause of the Absorption Lag. *American Journal of Botany*, *25*(2), 110–113. https://doi.org/10.2307/2436856

Kriedemann, P. E., Loveys, B. R., Fuller, G. L., & Leopold, A. C. (1972). Abscisic Acid and Stomatal Regulation 1. *Plant Physiology*, *49*(5), 842–847. https://doi.org/10.1104/pp.49.5.842

Kropp, H., Ogle, K., Vivoni, E. R., & Hultine, K. R. (2017). The Sensitivity of Evapotranspiration to Inter-Specific Plant Neighbor Interactions: Implications for Models. *Ecosystems*, *20*(7), 1311–1323. https://doi.org/10.1007/s10021-017-0112-5

Kwon, H., Law, B. E., Thomas, C. K., & Johnson, B. G. (2018). The influence of hydrological variability on inherent water use efficiency in forests of contrasting composition, age, and precipitation regimes in the Pacific Northwest. *Agricultural and Forest Meteorology*, *249*, 488–500. https://doi.org/10.1016/j.agrformet.2017.08.006

Lázaro-Nogal, A., Matesanz, S., Godoy, A., Pérez-Trautman, F., Gianoli, E., & Valladares, F. (2015). Environmental heterogeneity leads to higher plasticity in dry-edge populations of a semi-arid Chilean shrub: insights into climate change responses. *Journal of Ecology*, *103*(2), 338–350.

Lee, T. J., & Pielke, R. A. (1992). Estimating the Soil Surface Specific Humidity. *Journal of Applied Meteorology*, *31*(5), 480–484. https://doi.org/10.1175/1520-0450(1992)031<0480:ETSSSH>2.0.CO;2

Lehmann, P., Merlin, O., Gentine, P., & Or, D. (2018). Soil Texture Effects on Surface Resistance to Bare-Soil Evaporation. *Geophysical Research Letters*, *45*(19), 10,398-10,405. https://doi.org/10.1029/2018GL078803

Lévesque, M., Siegwolf, R., Saurer, M., Eilmann, B., & Rigling, A. (2014). Increased water-use efficiency does not lead to enhanced tree growth under xeric and mesic conditions. *New Phytologist*, *203*(1), 94–109. https://doi.org/10.1111/nph.12772

Li, X., Gentine, P., Lin, C., Zhou, S., Sun, Z., Zheng, Y., et al. (2019). A simple and objective method to partition evapotranspiration into transpiration and evaporation at eddy-covariance sites. *Agricultural and Forest Meteorology*, *265*, 171–182. https://doi.org/10.1016/j.agrformet.2018.11.017

Lin, C., Gentine, P., Huang, Y., Guan, K., Kimm, H., & Zhou, S. (2018). Diel ecosystem conductance response to vapor pressure deficit is suboptimal and independent of soil moisture. *Agricultural and Forest Meteorology*, *250–251*, 24–34. https://doi.org/10.1016/j.agrformet.2017.12.078

Loik, M. E., Breshears, D. D., Lauenroth, W. K., & Belnap, J. (2004). A multi-scale perspective of water pulses in dryland ecosystems: climatology and ecohydrology of the western USA. *Oecologia*, *141*(2), 269–281. https://doi.org/10.1007/s00442-004-1570-y

Maherali, H., Pockman, W. T., & Jackson, R. B. (2004). Adaptive Variation in the Vulnerability of Woody Plants to Xylem Cavitation. *Ecology*, *85*(8), 2184–2199. https://doi.org/10.1890/02-0538

Merlin, O., Stefan, V. G., Amazirh, A., Chanzy, A., Ceschia, E., Er-Raki, S., et al. (2016). Modeling soil evaporation efficiency in a range of soil and atmospheric conditions using a meta-analysis approach. *Water Resources Research*, *52*(5), 3663–3684. https://doi.org/10.1002/2015WR018233

Miralles, D. G., De Jeu, R. a. M., Gash, J. H., Holmes, T. R. H., & Dolman, A. J. (2011). Magnitude and variability of land evaporation and its components at the global scale. *Hydrology and Earth System Sciences*, *15*(3), 967–981. https://doi.org/10.5194/hess-15-967-2011

Miralles, D. G., Brutsaert, W., Dolman, A. J., & Gash, J. H. (2020). On the Use of the Term "Evapotranspiration." *Water Resources Research*, *56*(11), e2020WR028055. https://doi.org/10.1029/2020WR028055

Moran, M. S., Scott, R. L., Keefer, T. O., Emmerich, W. E., Hernandez, M., Nearing, G. S., et al. (2009). Partitioning evapotranspiration in semiarid grassland and shrubland ecosystems using time series of soil surface temperature. *Agricultural and Forest Meteorology*, *149*(1), 59–72. https://doi.org/10.1016/j.agrformet.2008.07.004

Morillas, L., Pangle, R. E., Maurer, G. E., Pockman, W. T., McDowell, N., Huang, C.-W., et al. (2017). Tree Mortality Decreases Water Availability and Ecosystem Resilience to

Drought in Piñon-Juniper Woodlands in the Southwestern U.S.: Tree Mortality in Semiarid Biomes. *Journal of Geophysical Research: Biogeosciences*, *122*(12), 3343–3361. https://doi.org/10.1002/2017JG004095

Nelson, J. A., Carvalhais, N., Cuntz, M., Delpierre, N., Knauer, J., Ogée, J., et al. (2018). Coupling Water and Carbon Fluxes to Constrain Estimates of Transpiration: The TEA Algorithm. *Journal of Geophysical Research: Biogeosciences*, *123*(12), 3617–3632. https://doi.org/10.1029/2018JG004727

Nelson, J. A., Pérez-Priego, O., Zhou, S., Poyatos, R., Zhang, Y., Blanken, P. D., et al. (2020). Ecosystem transpiration and evaporation: Insights from three water flux partitioning methods across FLUXNET sites. *Global Change Biology*, *26*(12), 6916–6930. https://doi.org/10.1111/gcb.15314

Niu, S., Xing, X., Zhang, Z., Xia, J., Zhou, X., Song, B., et al. (2011). Water-use efficiency in response to climate change: from leaf to ecosystem in a temperate steppe. *Global Change Biology*, *17*(2), 1073–1082. https://doi.org/10.1111/j.1365-2486.2010.02280.x

Novick, K. A., Ficklin, D. L., Stoy, P. C., Williams, C. A., Bohrer, G., Oishi, A. C., et al. (2016). The increasing importance of atmospheric demand for ecosystem water and carbon fluxes. *Nature Climate Change*, *6*(11), 1023–1027. https://doi.org/10.1038/nclimate3114

Ogle, K., Lucas, R. W., Bentley, L. P., Cable, J. M., Barron-Gafford, G. A., Griffith, A., et al. (2012). Differential daytime and night-time stomatal behavior in plants from North American deserts. *New Phytologist*, *194*(2), 464–476. https://doi.org/10.1111/j.1469-8137.2012.04068.x

Oleson, K., Lawrence, M., Bonan, B., Drewniak, B., Huang, M., Koven, D., et al. (2013). Technical description of version 4.5 of the Community Land Model (CLM). https://doi.org/10.5065/D6RR1W7M

Or, D., Lehmann, P., Shahraeeni, E., & Shokri, N. (2013). Advances in Soil Evaporation Physics—A Review. *Vadose Zone Journal*, *12*(4), vzj2012.0163. https://doi.org/10.2136/vzj2012.0163

Pérez-Priego, O., Katul, G., Reichstein, M., El-Madany, T. S., Ahrens, B., Carrara, A., et al. (2018). Partitioning Eddy Covariance Water Flux Components Using Physiological and Micrometeorological Approaches. *Journal of Geophysical Research: Biogeosciences*, *123*(10), 3353–3370. https://doi.org/10.1029/2018JG004637

Plummer, M. (2019). rjags: Bayesian Graphical Models using MCMC (Version 4-10). Retrieved from https://CRAN.R-project.org/package=rjags

Poggio, L., de Sousa, L. M., Batjes, N. H., Heuvelink, G. B. M., Kempen, B., Ribeiro, E., & Rossiter, D. (2021). SoilGrids 2.0: producing soil information for the globe with quantified spatial uncertainty. *SOIL*, *7*(1), 217–240. https://doi.org/10.5194/soil-7-217-2021

R Core Team. (2020). *R: A Language and Environment for Statistical Computing*. Vienna, Austria: R Foundation for Statistical Computing. Retrieved from https://www.R-project.org/

Reich, E., Samuels-Crow, K., Bradford, J., Litvak, M., Schlaepfer, D., & Ogle, K. (2023a). A semi-mechanistic model for partitioning evapotranspiration reveals scale-dependent moisture supply and demand controls water-use efficiency - all data, output, code, models [Data set]. https://doi.org/10.5281/zenodo.8213094

Reich, E., Samuels-Crow, K., Bradford, J., Litvak, M., Schlaepfer, D., & Ogle, K. (2023b, November 20). egreich/A-semi-mechanistic-model-for-partitioning-evapotranspiration: jgr-biogeo_pub (Version v1.0.0). Zenodo. https://doi.org/10.5281/zenodo.10161267

Reichstein, M., Falge, E., Baldocchi, D., Papale, D., Aubinet, M., Berbigier, P., et al. (2005). On the separation of net ecosystem exchange into assimilation and ecosystem respiration: review and improved algorithm. *Global Change Biology*, *11*(9), 1424–1439. https://doi.org/10.1111/j.1365-2486.2005.001002.x

Reynolds, J. F., Kemp, P. R., & Tenhunen, J. D. (2000). Effects of long-term rainfall variability on evapotranspiration and soil water distribution in the Chihuahuan Desert: A modeling analysis. *Plant Ecology*, *150*(1), 145–159. https://doi.org/10.1023/A:1026530522612

Rogiers, S. Y., Greer, D. H., Hatfield, J. M., Hutton, R. J., Clarke, S. J., Hutchinson, P. A., & Somers, A. (2012). Stomatal response of an anisohydric grapevine cultivar to evaporative demand, available soil moisture and abscisic acid. *Tree Physiology*, *32*(3), 249–261. https://doi.org/10.1093/treephys/tpr131

Rüdiger, C., Western, A. W., Walker, J. P., Smith, A. B., Kalma, J. D., & Willgoose, G. R. (2010). Towards a general equation for frequency domain reflectometers. *Journal of Hydrology*, *383*(3), 319–329. https://doi.org/10.1016/j.jhydrol.2009.12.046

Samuels-Crow, K. E., Ryan, E., Pendall, E., & Ogle, K. (2018). Temporal Coupling of Subsurface and Surface Soil CO2 Fluxes: Insights From a Nonsteady State Model and Cross-Wavelet Coherence Analysis. *Journal of Geophysical Research: Biogeosciences*, *123*(4), 1406–1424. https://doi.org/10.1002/2017JG004207

Samuels-Crow, K. E., Ogle, K., & Litvak, M. E. (2020). Atmosphere-Soil Interactions Govern Ecosystem Flux Sensitivity to Environmental Conditions in Semiarid Woody Ecosystems

Over Varying Timescales. *Journal of Geophysical Research: Biogeosciences*, *125*(8), e2019JG005554. https://doi.org/10.1029/2019JG005554

Scanlon, T. M., Schmidt, D. F., & Skaggs, T. H. (2019). Correlation-based flux partitioning of water vapor and carbon dioxide fluxes: Method simplification and estimation of canopy water use efficiency. *Agricultural and Forest Meteorology*, *279*, 107732. https://doi.org/10.1016/j.agrformet.2019.107732

Schlaepfer, D. R., Bradford, J. B., Lauenroth, W. K., Munson, S. M., Tietjen, B., Hall, S. A., et al. (2017). Climate change reduces extent of temperate drylands and intensifies drought in deep soils. *Nature Communications*, *8*(1), 14196. https://doi.org/10.1038/ncomms14196

Schlesinger, W. H., & Jasechko, S. (2014). Transpiration in the global water cycle. *Agricultural and Forest Meteorology*, *189–190*, 115–117. https://doi.org/10.1016/j.agrformet.2014.01.011

Schultz, H. r., & Stoll, M. (2010). Some critical issues in environmental physiology of grapevines: future challenges and current limitations. *Australian Journal of Grape and Wine Research*, *16*(s1), 4–24. https://doi.org/10.1111/j.1755-0238.2009.00074.x

Scott, R. L., & Biederman, J. A. (2017). Partitioning evapotranspiration using long-term carbon dioxide and water vapor fluxes: New Approach to ET Partitioning. *Geophysical Research Letters*, *44*(13), 6833–6840. https://doi.org/10.1002/2017GL074324

Scott, R. L., Huxman, T. E., Cable, W. L., & Emmerich, W. E. (2006). Partitioning of evapotranspiration and its relation to carbon dioxide exchange in a Chihuahuan Desert shrubland. *Hydrological Processes*, *20*(15), 3227–3243. https://doi.org/10.1002/hyp.6329

Scott, R. L., Knowles, J. F., Nelson, J. A., Gentine, P., Li, X., Barron-Gafford, G., et al. (2021). Water Availability Impacts on Evapotranspiration Partitioning. *Agricultural and Forest Meteorology*, *297*, 108251. https://doi.org/10.1016/j.agrformet.2020.108251

Stoy, P. C., El-Madany, T. S., Fisher, J. B., Gentine, P., Gerken, T., Good, S. P., et al. (2019). Reviews and syntheses: Turning the challenges of partitioning ecosystem evaporation and transpiration into opportunities. *Biogeosciences*, *16*(19), 3747–3775. https://doi.org/10.5194/bg-16-3747-2019

Sun, X., Wilcox, B. P., & Zou, C. B. (2019). Evapotranspiration partitioning in dryland ecosystems: A global meta-analysis of in situ studies. *Journal of Hydrology*, *576*, 123–136. https://doi.org/10.1016/j.jhydrol.2019.06.022

Tarin, T., Nolan, R. H., Medlyn, B. E., Cleverly, J., & Eamus, D. (2020). Water-use efficiency in a semi-arid woodland with high rainfall variability. *Global Change Biology*, *26*(2), 496–508. https://doi.org/10.1111/gcb.14866

Torrence, C., & Compo, G. P. (1998). A Practical Guide to Wavelet Analysis. *Bulletin of the American Meteorological Society*, *79*(1), 61–78. https://doi.org/10.1175/1520-0477(1998)079<0061:APGTWA>2.0.CO;2

Wei, Z., Yoshimura, K., Wang, L., Miralles, D. G., Jasechko, S., & Lee, X. (2017). Revisiting the contribution of transpiration to global terrestrial evapotranspiration. *Geophysical Research Letters*, *44*(6), 2792–2801. https://doi.org/10.1002/2016GL072235

Yamanaka, T., & Yonetani, T. (1999). Dynamics of the evaporation zone in dry sandy soils. *Journal of Hydrology*, *217*(1), 135–148. https://doi.org/10.1016/S0022-1694(99)00021-9

Zahn, E., Bou-Zeid, E., Good, S. P., Katul, G. G., Thomas, C. K., Ghannam, K., et al. (2022). Direct partitioning of eddy-covariance water and carbon dioxide fluxes into ground and plant components. *Agricultural and Forest Meteorology*, *315*, 108790. https://doi.org/10.1016/j.agrformet.2021.108790

Zhang, Q., Ficklin, D. L., Manzoni, S., Wang, L., Way, D., Phillips, R. P., & Novick, K. A. (2019). Response of ecosystem intrinsic water use efficiency and gross primary productivity to rising vapor pressure deficit. *Environmental Research Letters*, *14*(7), 074023. https://doi.org/10.1088/1748-9326/ab2603

Zhang, W., Koch, J., Wei, F., Zeng, Z., Fang, Z., & Fensholt, R. (2023). Soil Moisture and Atmospheric Aridity Impact Spatio-Temporal Changes in Evapotranspiration at a Global Scale. *Journal of Geophysical Research: Atmospheres*, *128*(8), e2022JD038046. https://doi.org/10.1029/2022JD038046

Zhou, S., Yu, B., Zhang, Y., Huang, Y., & Wang, G. (2016). Partitioning evapotranspiration based on the concept of underlying water use efficiency. *Water Resources Research*, *52*(2), 1160–1175. https://doi.org/10.1002/2015WR017766

References From the Supporting Information

Albergel, C., Balsamo, G., de Rosnay, P., Muñoz-Sabater, J., & Boussetta, S. (2012). A bare ground evaporation revision in the ECMWF land-surface scheme: evaluation of its impact using ground soil moisture and satellite microwave data. *Hydrology and Earth System Sciences*, *16*(10), 3607–3620. https://doi.org/10.5194/hess-16-3607-2012

Allen, R. G., Pereira, L. S., Raes, D., & Smith, M. (2000). *Crop evapotranspiration: guidelines for computing crop water requirements* (repr). Rome: Food and Agriculture Organization of the United Nations.

Bolton, D. (1980). The Computation of Equivalent Potential Temperature. *Monthly Weather Review*, *108*(7), 1046–1053. https://doi.org/10.1175/1520-0493(1980)108<1046:TCOEPT>2.0.CO;2

Brisson, N., & Perrier, A. (1991). A semiempirical model of bare soil evaporation for crop simulation models. *Water Resources Research*, *27*(5), 719–727. https://doi.org/10.1029/91WR00075

Choudhury, B. J., Reginato, R. J., & Idso, S. B. (1986). An analysis of infrared temperature observations over wheat and calculation of latent heat flux. *Agricultural and Forest Meteorology*, *37*(1), 75–88. https://doi.org/10.1016/0168-1923(86)90029-8

Clapp, R. B., & Hornberger, G. M. (1978). Empirical equations for some soil hydraulic properties. *Water Resources Research*, *14*(4), 601–604. https://doi.org/10.1029/WR014i004p00601

Cosby, B. J., Hornberger, G. M., Clapp, R. B., & Ginn, T. R. (1984). A Statistical Exploration of the Relationships of Soil Moisture Characteristics to the Physical Properties of Soils. *Water Resources Research*, *20*(6), 682–690. https://doi.org/10.1029/WR020i006p00682

Foken, T. (2006). 50 Years of the Monin–Obukhov Similarity Theory. *Boundary-Layer Meteorology*, *119*(3), 431–447. https://doi.org/10.1007/s10546-006-9048-6

Lee, T. J., & Pielke, R. A. (1992). Estimating the Soil Surface Specific Humidity. *Journal of Applied Meteorology*, *31*(5), 480–484. https://doi.org/10.1175/1520-0450(1992)031<0480:ETSSSH>2.0.CO;2

Merlin, O., Stefan, V. G., Amazirh, A., Chanzy, A., Ceschia, E., Er-Raki, S., et al. (2016). Modeling soil evaporation efficiency in a range of soil and atmospheric conditions using a meta-analysis approach. *Water Resources Research*, *52*(5), 3663–3684. https://doi.org/10.1002/2015WR018233

Monin, A. S., & Obukhov, A. M. (1954). Basic laws of turbulent mixing in the surface layer of the atmosphere. *Tr. Akad. Nauk SSSR Geophiz. Inst.*, *24*(151), 163–187.

Oleson, K., Lawrence, M., Bonan, B., Drewniak, B., Huang, M., Koven, D., et al. (2013). Technical description of version 4.5 of the Community Land Model (CLM). https://doi.org/10.5065/D6RR1W7M

Philip, J. R., & De Vries, D. A. (1957). Moisture movement in porous materials under temperature gradients. *Eos, Transactions American Geophysical Union*, *38*(2), 222–232. https://doi.org/10.1029/TR038i002p00222

Sakaguchi, K., & Zeng, X. (2009). Effects of soil wetness, plant litter, and under-canopy atmospheric stability on ground evaporation in the Community Land Model (CLM3.5). *Journal of Geophysical Research: Atmospheres*, *114*(D1). https://doi.org/10.1029/2008JD010834

Sellers, P. J., Heiser, M. D., & Hall, F. G. (1992). Relations between surface conductance and spectral vegetation indices at intermediate (100 m2 to 15 km2) length scales. *Journal of Geophysical Research: Atmospheres*, *97*(D17), 19033–19059. https://doi.org/10.1029/92JD01096

Stefan, V. G., Merlin, O., Er-Raki, S., Escorihuela, M.-J., & Khabba, S. (2015). Consistency between In Situ, Model-Derived and High-Resolution-Image-Based Soil Temperature Endmembers: Towards a Robust Data-Based Model for Multi-Resolution Monitoring of Crop Evapotranspiration. *Remote Sensing*, *7*(8), 10444–10479. https://doi.org/10.3390/rs70810444

Yang, Y., Guan, H., Batelaan, O., McVicar, T. R., Long, D., Piao, S., et al. (2016). Contrasting responses of water use efficiency to drought across global terrestrial ecosystems. *Scientific Reports*, *6*(1), 23284. https://doi.org/10.1038/srep23284